Engineering Failure Analysis 18 (2011) 1308–1321

Contents lists available at ScienceDirect

Engineering Failure Analysis

journal homepage: www.elsevier.com/locate/engfailanal

Failure analysis and effects of redesign of a polypropylene yarn twisting machine

B. Tadic [a], P.M. Todorovic [a], Dj. Vukelic [b,*], B.M. Jeremic [a]

[a] University of Kragujevac, Faculty of Mechanical Engineering, Department for Production Engineering, 34000 Kragujevac, Serbia
[b] University of Novi Sad, Faculty of Technical Sciences, Department for Production Engineering, 21000 Novi Sad, Serbia

ARTICLE INFO

Article history:
Received 17 November 2010
Received in revised form 21 March 2011
Accepted 28 March 2011
Available online 1 April 2011

Keywords:
Failure analysis
Vibration
Fracture
Design
FEM analysis

ABSTRACT

Presented in this paper are the results pertaining to technical condition diagnostics, redesign, and analysis of its effects for a complex mechanical system of a polypropylene yarn twisting machine. Twelve twisting machines were installed on a polypropylene yarn production line. Due to design flaws and manufacturing errors, the winches were soon prone to failures and an unacceptable level of vibrations. Owing to insufficient structure rigidness, errors in design, manufacturing errors, and a high level of vibrations, the majority of twisting machines developed cracks in their foundation framework. FEM analysis was used with experimentally measured displacements in the crack zone to define stress distribution. Also shown in this paper is the method for measurement and analysis of the vibration signal during the winch run-up, with the aim to determine resonance zones and a condition analysis of the twisting machine framework. In order to make the winches fully operational, a redesign of the mechanical structure was performed. The level of vibration was measured again at the characteristic framework parts, and FEM analysis of the foundation framework was used to analyse the effects of the redesign. The vibration measurements and the results of FEM analysis proved that the redesign was successful, showing that the measures undertaken made this system fully operational again.

1. Introduction

The determination of complex technical systems and the causes of the breakdown of their components is a multifaceted problem which requires an interdisciplinary approach [1]. Engineering analyses (FEM analysis, modal analysis, thermal analysis, and other methods) sometimes fail to provide sufficient information for a valid conclusion as to the cause of a breakdown. For this reason, the analysis of complex, real-life designs sometimes requires a combination of numerical and experimental methods. Some typical examples of such combination of methods in analysis of complex mechanical structures are given by Ref. [2–5]. This paper reviews the results of investigation on diagnostics of real-life mechanical structures and their proposed redesign. Trebuna et al. [2] analysed a press frame failure with the aim to propose an optimal variant of its strengthening. Witek et al. [3] described the fracture problem of the turbine casing of a helicopter engine. Goksenli and Eryurek [4] analysed a failure analysis of an elevator drive shaft. Poursaeidi and Mohammadi Arhani [5] presented the results of a failure investigation of an auxiliary steam turbine in a power plant. One common feature of these investigations is that their stress analysis of the mechanical structure is based on the known load values, which is not the case in this study.

Many rotating machines may be considered as consisting of three major parts: the rotor, the bearings and the foundations [6]. With the majority of rotating machines the influence of foundations on machine dynamics is very important. With a

* Corresponding author. Tel.: +381 21 485 23 26; fax: +381 21 454 495.
E-mail address: vukelic@uns.ac.rs (Dj. Vukelic).

1350-6307/$ - see front matter © 2011 Elsevier Ltd. All rights reserved.
doi:10.1016/j.engfailanal.2011.03.020

dramatic increase of turbo generator unit size in the 1960s and 70s, machines using flexible rotors became prevalent and at the same time there was a trend to support machines on lightweight fabricated steel structures rather than the massive concrete supports of previous eras [7]. Lees et al. [7] also point out that the newer steel foundations tend to be low tuned, which means they have several natural frequencies below the machine's operating speed and consequently have substantial influence on the overall behaviour.

Theoretical modelling of a rotating machinery foundation is a difficult task due to its complicated configuration and interaction with the surrounding environment. The finite element (FE) method is established as the pre-eminent approach to problems in structural dynamics and for a time it was widely believed that once suitable codes were developed then the computation of machine behaviour would be a relatively straightforward matter. However, as our understanding has increased, it has become clear that some fundamental issues need addressing [7]. Various factors such as uncertain material properties, involved structural details, connections to the surrounding environment, and even the actual assembly of the foundation and machine elements may affect its dynamic characteristics. A practical and in some cases the only feasible approach is to identify the characteristic parameters experimentally [8].

Over the decades, vibration based identification of faults, such as rotor unbalance, rotor bend, cracks, rubs, misalignment, have been well developed and implemented in practice [6,9]. A large number of papers show that the condition of flexibly supported rotating machinery, in a wider sense, or, more specifically, the condition of the foundation of machinery, can be assessed by measuring vibration data during the machine run-up or run-down period.

Shown in this paper is the method of measurement and analysis of vibration signals during run-up of the tested rotating machine, in order to determine the resonance zones, and analyse the state of the twisting machine's mechanical framework before and after the redesign. Also presented are the results of combined experimental and numerical methods which were used to determine stresses in critical zones of the twisting machine's mechanical framework.

2. Description and condition analysis of the investigated technical system

The twisting machine (Fig. 1) operates in a production line for polypropylene (PP) binder. The role of the 12 winches within this system is to roll the formed PP strips into a yarn with the required denier number. From the aspect of kinematics and machine dynamics, the twisting machine is a complex mechanical system.

Shown in Fig. 2 are the kinematics diagram and assembly of the cradle, epicycles, and yarn twisting knives which are located in the internal section of the foundation framework. "E1", "E2", and "E3" designate critical zones of the foundation framework which are analysed in detail later in this paper.

Unlike other production line components, from the very beginning of their operational life, the twisting machines showed a high rate of bearing failures and a high level of vibrations. In order to solve the problem on the twisting machines, a number of interventions were undertaken. All of them improved the system to some extent, but productivity was still below 50% of the nominal.

Videoscopic examination revealed cracks in foundations (lateral support plates) of 8 out of 12 twisting machines which operate within the PP yarn production line (Fig. 3a). The cracks were partially healed by the owner, by welding. An analysis of the twisting machine foundation framework, and videoscopic examination, revealed the following:

- twisting machine foundation is designed as a light welded framework,
- lateral support plates, 12 mm thick, are weakened by trapezoidal openings which allow evacuation of dust from the foundation interior,

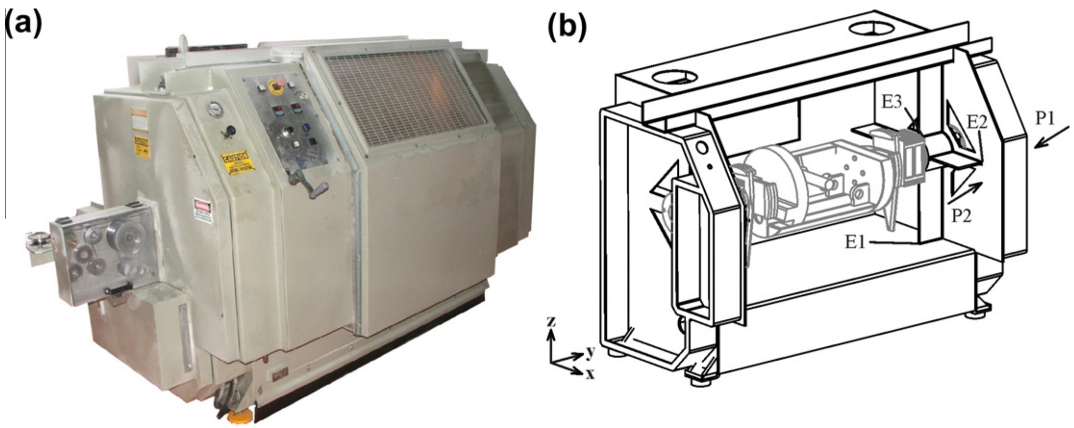

Fig. 1. Twisting machine. (a) Photo. (b) CAD model of the foundation framework with designated critical zones "E1", "E2", and "E3". Overall foundation dimensions: 2417 × 1644 × 1160 mm; foundation mass: 1099 kg.

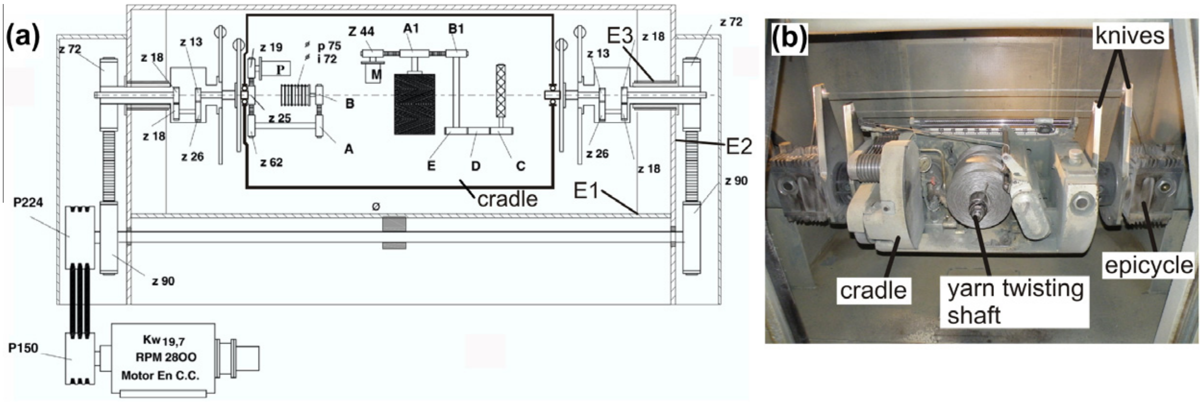

Fig. 2. Twisting machine. (a) Kinematics diagram. (b) Photo of the cradle, epicycles, and yarn twisting knives.

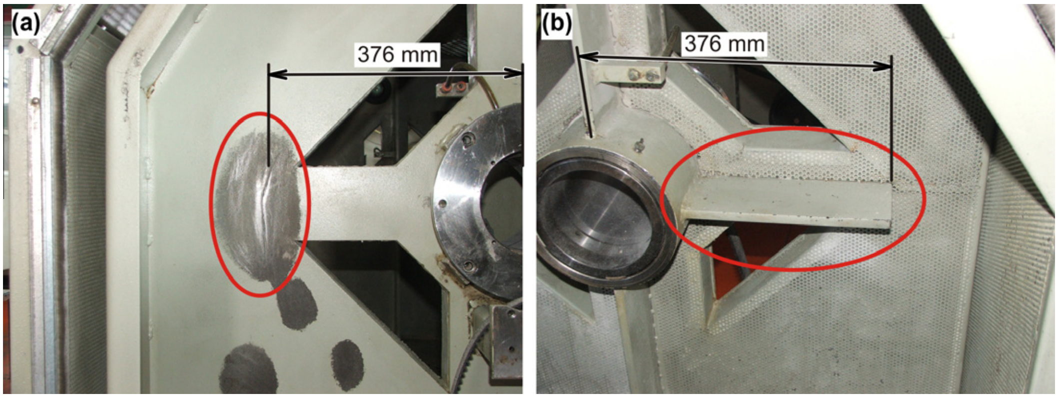

Fig. 3. Typical cracks in zone "E2" on the twisting machine foundation framework. (a) Lateral side, view "P2" (from Fig. 1b). (b) The zone of shortened reinforcement rib on the internal side, view "P1" (from Fig. 1b).

- on the inner side of the foundation interior the reinforcement rib is discontinued exactly opposite the crack zone (Fig. 3b).

The authors began their analysis from the fact that the operating stress levels exceeded the allowed values in the crack zone. It was necessary to first establish the types and magnitudes of loads which lead to crack occurrence. With this in mind, the following was established:

(a) In an ideal case of axial alignment of all bearings, and supposing that the system is perfectly rigid, the cradle (Fig. 2b) acts as a pendulum. Due to numerous manufacturing errors which pertain to kinematics and geometrical axes misalignment, and system elasticity in general, the cradle assembly's motion is complex. Presented in Fig. 4. are:
  - possible manufacturing errors (Fig. 4a),
  - possible position of cradle within the foundation framework assembly (Fig. 4b),
  - possible trajectories of the cradle mass centre (Fig. 4c), and
  - photo of worn epicycle shaft journal (Fig. 4d).

Some of the possible manufacturing errors are (Fig. 4a): e_1 – misalignment between the axes of central bearing; e_2 and e_3, – misalignment between the axis of rotation of the epicycle shaft, and the axis of the central bearing, and e_4 – misalignment between bearing axes on the cradle. The central (A_1 and A_2) and cradle bearing supports (B_1 and B_2) use roller bearings with increased radial clearance (class C3). These bearings were used with the intention to compensate for possible thermal effects, as well as some manufacturing errors. However, to a certain extent, the increased radial clearance shifts the cradle's centre of gravity in a radial direction. Due to the presence of manufacturing errors and the clearance, the rotation of the epicycle shaft puts the cradle into complex motion. In other words, the cradle's centre of mass travels along a complex trajectory relative to the axis of rotation (Fig. 4c). This generates inertial forces which load the lateral support plates via the epicycle shaft. Using elastic lines, Fig. 4b shows the deformed position of the cradle assembly, epicycle assembly, and the lateral support plates. The position of the cradle's centre of mass relative to rotation axis is defined by coordinate $\rho(\varphi)$ (see Fig. 4c). Generally, this coordinate, and the inertial force, depend on manufacturing errors, bearing clearance, stiffness of framework components in various directions, angular velocity of drive shafts, cradle mass, temperature field, and other factors.

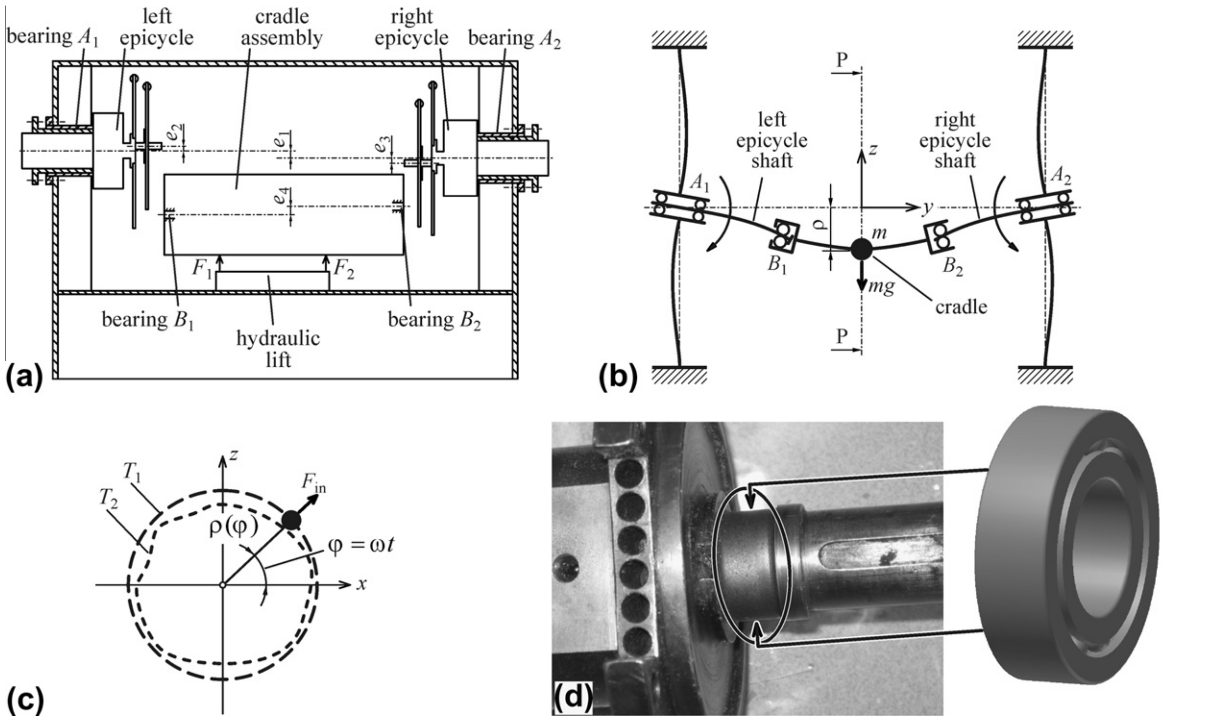

Fig. 4. (a) Manufacturing errors. (b) Cradle position described by elastic lines. (c) Possible trajectories of cradle mass centres T1 and T2. (d) Photo of worn epicycle shaft journal.

Measurements showed that the axis of epicycle shaft rotation has a misalignment e_2 of 0.24 mm relative to the central bearing axis, which is very high. To illustrate this, below is given an approximation of the inertial force which corresponds to misalignment of 0.24 mm, 150 kg mass of cradle assembly, and a drive shaft speed of $n = 2200$ RPM (which is approximately 90% of the machine's nominal capacity). The generated inertial force can be calculated as [1]:

$$F_{\text{in}} = m \cdot \rho \cdot \omega^2 = 150 \cdot \frac{0.24}{1000} \cdot \left(\frac{\pi \cdot n}{30}\right)^2 = 1908.8\ \text{N} \tag{1}$$

where ω is the calculated angular speed.

Based on this example, which took into consideration just one of the measured manufacturing errors, it is evident that these errors represent a serious threat to the system's reliability.

(b) An obvious example of high loads on the cradle bearing – and, consequently, the entire twisting machine foundation framework – is the fact that in some twisting machines the cradle bearing gets blocked and the inner bearing ring begins to slip along the journal (Fig. 4d). Beside mechanical damage, this occurrence generates an additional thermal load through friction heat.

(c) During assembly of the cradle, and both epicycles into the twisting machine foundation framework, due to errors e_1–e_4 (Fig. 4a), additional preloads are generated on the lateral support plates. It should be noted that cradle bearings (B_1 and B_2) are not capable of significantly compensating the angular misalignments of the epicycle shaft, which greatly influences the magnitude of the preloads.

(d) vFor reasons stated above, it can be assumed that there are significant displacements and stresses on the lateral support plates of the central bearing (A_1 and A_2), as they have relatively little stiffness. On the side of the cracked lateral plate, the epicycle shaft is supported only by a radial bearing (bearing B_2; Fig. 4b). Such bearing design – radial–axial bearing in support B_1, and radial bearing in support B_2 (Fig. 4b) – is motivated by necessity to reduce thermal loads. It is evident that the cracked lateral support plate is loaded in a radial direction by the epicycle shaft, while the influence of the axial load can be disregarded, considering the bearing design. This assumption is crucial for the FEM analysis discussed later.

(e) The system is also subject to thermal loads. In the twisting machine system the heat is generated primarily due to conversion of mechanical into thermal energy. The source of thermal energy is the friction between the large number of contact pairs (bearings, gears, belts, etc.). Shown in Fig. 5 are infrared (IR) images of temperature fields generated by IR camera Flir P640. Considering the levels of temperatures, one concludes that the crack zone was not exposed to temperatures which could have caused structural changes of the material and the diminishing of its dynamic strength. The influence of temperature is nevertheless negative, primarily because it necessitates larger radial clearances, which results in the shift of the cradle mass centre, and larger inertial forces.

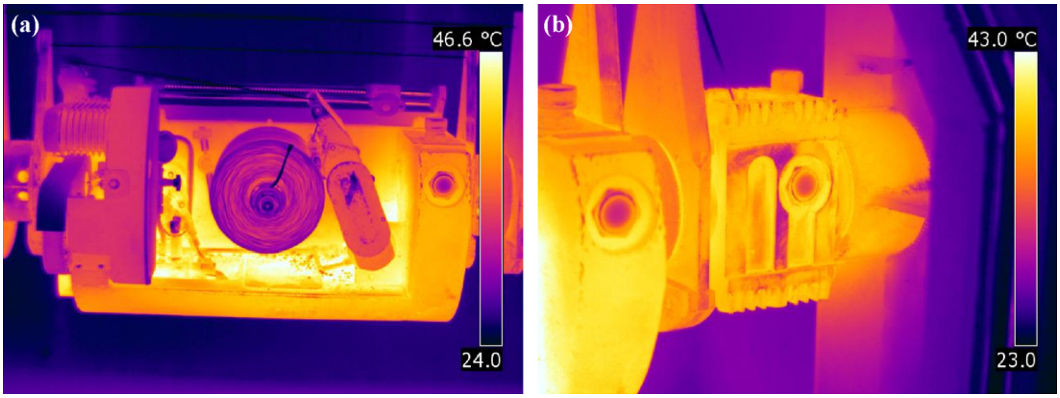

Fig. 5. IR image of temperature fields inside twisting machine. (a) The cradle. (b) The epicycle and bearing A_2.

(f) The cradle which, as previously stated, performs complex motion over, generally, unknown trajectories (Fig. 4c), carries a large number of assemblies. The cradle is driven by the epicycle shaft, while a system of mechanical and hydraulic transfer of energy (gears, belt drives, hydromotor, reservoir, pipelines, and other components) drives the yarn twisting shaft, yarn stretching mechanism, yarn guiding system, and other components (Fig. 2a). All these components and assemblies are mounted on the cradle, and possess their own motion dynamics. This results in dynamic forces which are transferred onto lateral support plates via the epicycle shaft. It was not possible to create a complete dynamic model of such a complex dynamic system, due to the following:
- the user of this equipment is not in possession of complete design documentation, but just a small fragment of maintenance documentation,
- thorough dynamic modelling would practically require complete reverse engineering of the twisting machine which, given the situation, would not be practical, and
- financial losses caused by the breakdown of the PP yarn production line were very high, which demanded that the problems be solved in the shortest possible time.

with this in mind, the authors assumed the following:

- Generally, the values of forces generated during machine operation which load the foundation framework are not known.
- Most of the loading received by the lateral support plates is transferred from the epicycle shaft.
- The load is of varying direction and sense, and acts mostly in the *XZ*-plane (Fig. 1b).
- Due to the cradle bearing design, part of the axial load (*Y*-axis direction) is transferred via the epicycle shaft onto the lateral support plate which does not feature any cracks.
- Higher stability of the lateral support plate which had no visible cracks, stems from the reinforcement, i.e., the uncut reinforcement rib, as well as the additional stiffening by the prismatic welded elements, forming the box which houses part of the hydraulic and electronic components.
- The forces which act in the axial direction (*Y*-axis) are of secondary importance to the generation of cracks. Compared to the forces acting in the *XZ*-plane, they are of little consequence. Besides, the axial forces act on the reinforced lateral support plate which is not weakened by cracks. Considering the theoretical point in which the axial force acts, its contribution to the total load of the lateral support plate with cracks is negligible.

The above assumptions shall be applied to the problem of defining the critical zones of the twisting machine foundation framework. Attention is focused on zone "E2" on the cracked lateral support plate, as well as on determination of critical stresses in that zone. For this purpose, the measurements of radial (*Y*-axis) displacements taken in the crack zone, were used as input into the FEM analysis. The radial displacements in the crack zone were calculated by the integration of the vibration velocity signal from the crack zone of the lateral support plate. Simulation of loads in the *XZ*-plane of various directions and magnitudes, allowed determination of direction and minimum magnitude of force which acts on the epicycle shaft and causes measured displacements in the crack zone. The same method was used to determine the stresses in the crack zone of the lateral support plate.

3. Measurement results for radial displacement in the crack zone

The axial displacement in the direction of the *Y*-axis in the crack zone of the lateral support plate (Fig. 6) was determined by numerical integration of the signal of vibration velocity in that zone. The method used for vibration velocity measurement is described in detail in Section 5. Thus calculated, the axial displacement in the "E2" crack zone was used as input and boundary value for FEM analysis and stress determination in that zone.

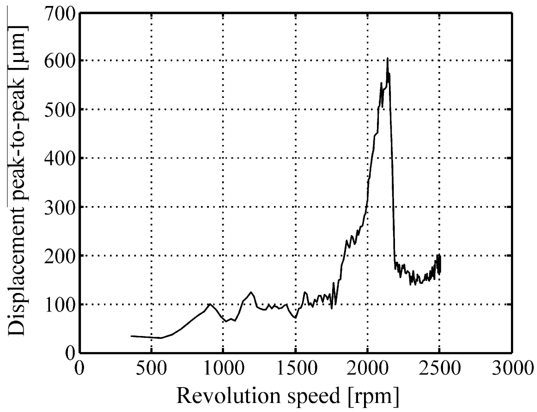

Fig. 6. Vibrations expressed as peak-to-peak axial displacement in the crack zone of the lateral support plate.

Maximum axial displacements of 605 μm peak-to-peak, i.e., approximately ±0.3 mm (Fig. 6) corresponds to 2140 RPM, which is approximately 90% of the nominal twisting machine capacity. The conducted FEM analysis was aimed at determining the load and stresses in the crack zone which correspond to maximum displacement.

4. Results of FEM analysis

FEM analysis was conducted in Autodesk Inventor Simulation software. Shown in Fig. 7a and b is FE mesh with 200,688 tetrahedral elements, and 351,931 nodes. As can be seen from Fig. 7b, the mesh is refined in the crack zone and consists of a significantly larger number of FEs than the rest of the model. The twisting machine is tied to the ground by fixed supports (four foot supports) which constitutes a boundary condition for FEM analysis. The load is transferred from the epicycle shaft onto the internal wall of the collets which are fixed to the ribs, and lateral support plates. Mechanical characteristics of the foundation framework material – structural steel S 235 JRG2 [10] – used in FEM analysis are: Young modulus, $E = 210$ GPa, the Poisson ratio, $\nu = 0.3$, and density, $\rho = 7800$ kg/m^3. Fig. 7a also shows one of the simulated directions of the load, which adds up to cradle weight, and loads the main bearings A_1, and A_2 (Fig. 4a).

The simulation of various load directions in the radial *XZ*-plane established that the static force of approximately 8 kN causes the maximum displacement measured in the crack zone. The results of FEM analysis indicate that the simulated direction, and intensity of this load causes significant stress concentration in the very crack zone. Shown in Fig. 8a, and b are distributions of Von-Mises stress in the crack zone of the lateral support plate, the central bearing zone, and the zone of the vertical rib support (zones "E1", "E2", and "E3"). The calculated stress in the crack (Fig. 8b) equals 169.7 MPa.

The simulation of various load directions also leads to the conclusion that the stress in "E3" zone is largest for the shown direction, equalling 49 MPa. The stress in "E1" zone is largest when the simulated load has a vertical direction and coincides with cradle gravity force, equalling 10.79 MPa. Graphical representation of the results of this calculation are omitted for the sake of brevity and their lesser importance.

Shown in Fig. 9 is the axial displacement field in the direction of the *Y*-axis. Based on the calculated stresses and displacements, one concludes that the stress in the crack of 169.7 MPa corresponds to *Y*-axis displacement of −0.297 mm (Fig. 9). The displacement of ±0.3 mm was also calculated based on vibration velocity measurements (Fig. 6).

The conducted FEM analysis reveals that the crack zone is the most critical section of the foundation framework. Stresses in this zone reach 169.7 MPa. The loads simulated in the analysis were static and as such could not match the character of dynamic loads which occur in reality. However, regardless of the load type, the stresses obtained by FEM analysis were based on displacements measured in the crack zone, and cannot significantly diverge from the real values of maximum stresses the material in the crack zone was exposed to. Especially high stresses were obtained for the cyclic dynamic load, considering the dynamic properties of the foundation framework material which is structural steel, S 235 JRG2 [10]. A characteristic for this type of steel is that its dynamic strength diminishes under alternate dynamic loads. After 50,000 load cycles, it suddenly drops from 300 MPa to 200 MPa. After 10^6 load cycles, the dynamic strength of this steel under alternate dynamic loads equals 150–165 MPa [11]. The exact operating time is not known for the discussed twisting machine. However, considering the level of production, as well as the character of the dynamic load, and the fact that the machine had already been in service prior to delivery, it can be said with certainty that the number of load cycles exceeded the 10^6 limit.

It is well known that metal materials are susceptible to fatigue, and once the cracks appear, even smaller loads cause their growth in most cases [12]. The fatigue phenomenon includes the gradual growth of cracks until the remaining material yields under stress. Among the number of fatigue mechanisms are a high number of load cycles (usual limit is above 10^6 cycles), a low number of load cycles (usual limit is below 10^5 cycles), thermal influence, corrosion, creeping, and other influences [13]. In spite of the fact that these mechanisms are well known, the phenomenon of initiation and growth of cracks is

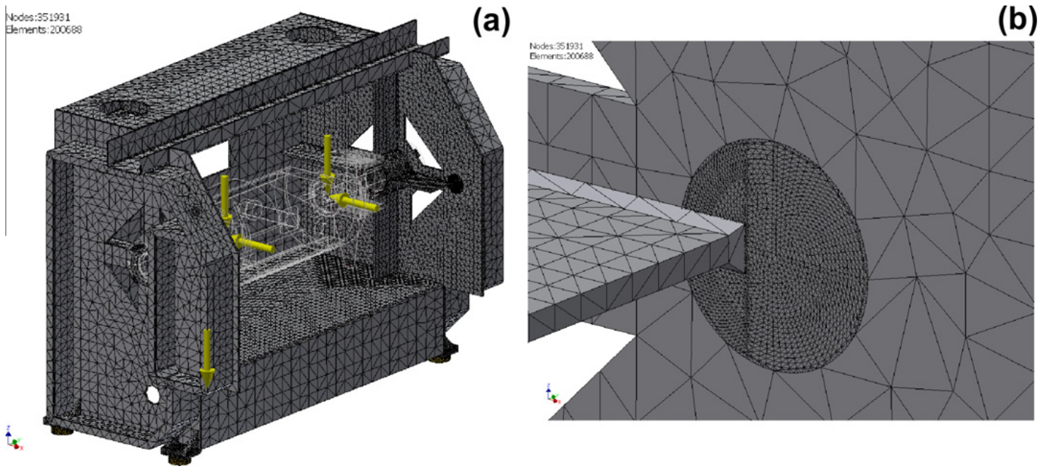

Fig. 7. CAD model of the twisting machine foundation framework. (a) Mesh of finite elements with a number of nodes and elements designated. (b) FE mesh in the crack zone (''E2'').

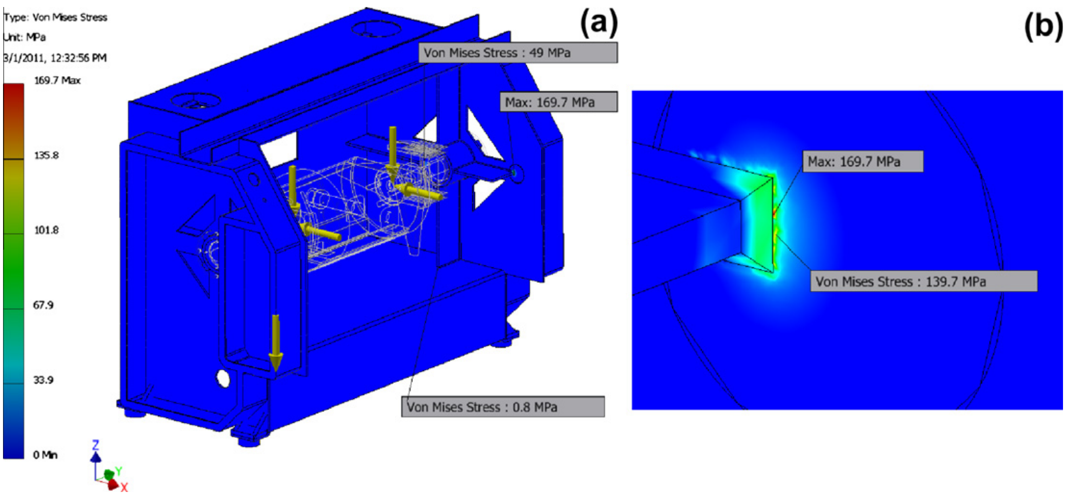

Fig. 8. (a) Distribution of Von-Mises stress in the twisting machine foundation framework. (b) A detail of the stress concentration zone.

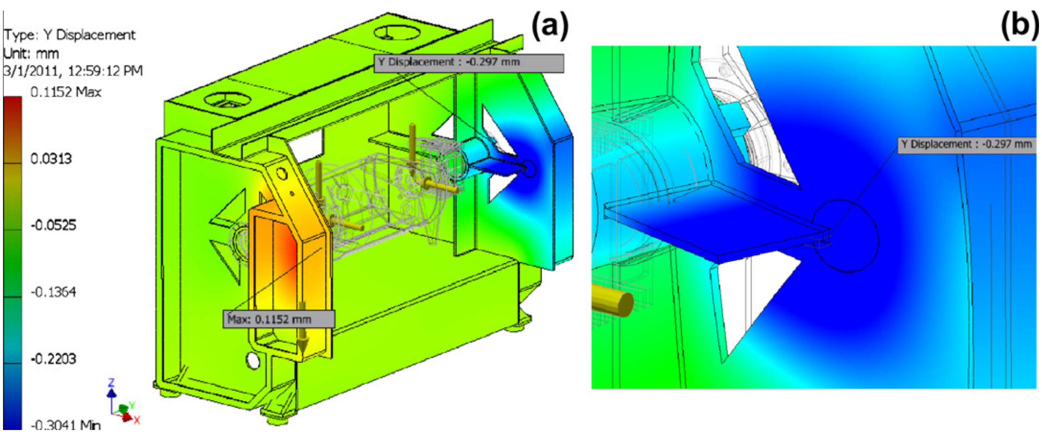

Fig. 9. (a) Displacement field in Y-axis direction. (b) Detail of displacement field in the crack zone.

more complex, especially because, in reality, it can include several mechanisms, i.e., joint action of cyclic structural and thermal loads. The twisting machines are high-productivity machines which operate under a significant level of structural loads, and lower level of thermal loads, and in environments, where tribo-mechanical systems are exposed to intensive dust pollution, originating from the polypropylene manipulation process.

Basically, cracks can extremely deteriorate the performance of twisting machines which have low-carbon structural steel foundations and support large masses (gear trains, hydraulic installations, and other moving parts) which rotate at relatively high speeds. It is clear that cracks can be dangerous not only from a structural point of view, but can endanger operational safety as well. Since the foundations we consider in this paper are welded frameworks, their behaviour – dynamic stability of the framework, partially depends on the remaining stresses, stress concentration, quality of welded joints, and other factors which cannot be precisely calculated and taken account of.

The considered foundation framework showed instability in exploitation, and the cracks rendered it practically unusable. Framework reinforcement was necessary, and it was to be done in a cramped space, and within a limited time. Based on the FEM analysis, the stresses in the crack zone were higher than the dynamic strength of material. This indicated the need for reinforcement of the foundation framework. The basic idea of redesign was to unload the zone, where the crack occurred, by creating additional framework support, while transferring a major part of the load onto the lower framework which features the concentration of reinforcement elements.

5. Theoretical foundations and a description of the method for vibration measurement

Vibration signals from rotating machinery contain important information for the diagnosis of machine faults, and it has been widely recognised that vibration signal analysis is an effective tool for condition monitoring (CM). One of the key characteristics of vibration signals from rotating machinery is the strong influence that the rotational speed has on the observed signals. Non-constant rotational speed leads to a non-stationary measured signal, which then becomes difficult to interpret. To deal with this, order tracking techniques have been developed. One of the main advantages of order tracking over traditional vibration monitoring techniques lies in its ability to clearly identify non-stationary vibration data, and to a large extent exclude the influences of the varying rotational speed [14].

In this paper, vibration measurement was used to determine the resonance zones of the twisting machine, and therefore measurements took place during run-up, i.e., during non-constant rotational speed. Also of interest was to determine the speed-related vibration signal components, which is why the method of computed order tracking (COT) was used for signal analysis. This is a frequency analysis method that uses multiples of the running speed (orders), instead of absolute frequencies (Hz), as the frequency base. In this way, vibration components that are proportional to multiples of the running speed can be easily identified [15].

The order tracking requires sampling of the vibration signal at constant angular increments. A COT method samples vibration data at a constant rate (i.e., uniform Δt), and then uses some numerical methods to resample the vibration data at a constant angular increment (i.e., uniform $\Delta\theta$). The COT method first records data at constant Δt increments, and then resamples this signal to provide the desired constant $\Delta\theta$, based on a key-phasor signal which typically generates one pulse per shaft revolution [15]. By using the key phasor it is also possible to locate the beginning and the end of rotations and to measure their time of duration [16]. In this paper, uniformly time-sampled vibration data are digitally resampled to the angle domain using the key-phasor signal and the cubic spline interpolation algorithm. Cubic spline interpolation is described in more detail in Refs. [17,18].

A block diagram of the equipment for measurement and analysis of the vibrations of the twisting machine is shown in Fig. 10. The vibrations are measured simultaneously with two BK 4391 piezoelectric charge accelerometers. These accelerometers have a frequency range from 0.1 Hz to 10 kHz and a charge sensitivity of 9.8 pC/g. Acceleration signal integration was done with a vibration signal conditioner with a 1 kHz anti-aliasing low pass filter and a velocity vibration signal was obtained. The key phasor was placed on the drive shaft. The eight analogue input channel simultaneous sampling data acquisition (DAQ) module with 16-bit resolution was used for discretization of the signal from the key phasor and two vibration sensors.

Uniformly time-sampled vibration data were digitally resampled to the angle domain ($\Delta t \rightarrow \Delta\theta$) by using the cubic spline algorithm. To be able to resample data, a high resolution RPM vector is needed, preferably with the same sampling frequency

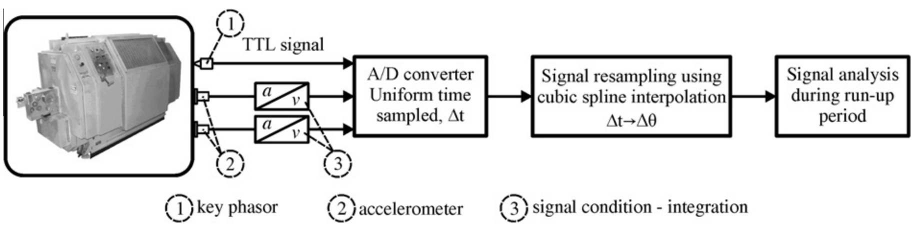

Fig. 10. Flow diagram of measurement and analysis of vibrations on a twisting machine.

as the vibration signal [19]. Nevertheless, at high frequencies, when analysing orders close to the Nyquist frequency, the standard sampling factor of 2.56 used by most recording devices is not adequate [19]. With this in mind, the signal data were measured with a sampling rate of 10 kHz which is somewhat above the Nyquist criterion.

A typical example of accelerometer readings in ‘‘E3’’ zone during run-up is shown in Fig. 11a. It is clear from this diagram that the resonance zone appears between 20 s and 22 s after machine startup.

Fig. 11b shows a segment of the vibration signal between 0 s and 5 s after machine startup, as well as the key-phasor signal which represents a one-per-revolution event. The key-phasor signal defines the start of each single rotation of the twisting machine, so it is possible to calculate the duration of every rotation, as well as to draw the diagram of RPM change during run-up (Fig. 12a). The total run-up time is defined by the technical characteristics of the drive engine and control electronics.

Knowing the exact moments of the start and end for each rotation, it is possible to define the root mean square (rms) of vibrations during machine run-up (Fig. 12b). The resonance zone clearly shows in the region of 2140 RPM. Similar diagrams were obtained at other measurement spots. This region corresponds to 90% of the full load of the twisting machine, which, considering the production line capacity, is the recommended operating regime. Due to high vibration levels, this regime was avoided and RPMs below 2140 were used in operation.

In order to determine the cause of high vibration levels it was necessary to analyse the signal in the frequency domain. The Fast Fourier Transform (FFT), as a widely used digital signal processing (DSP) method, allows each vibration component to be shown as a discrete frequency peak in the frequency spectrum. The dominant frequencies in the frequency spectrum are often related to a particular machine component or process in the system [15]. As a result of non-constant rotational speed, the frequency spectrum could be useless, because higher frequency components could be spread over several lines [16,20,21]. To prevent the mentioned limitation, some of the signal's resampling techniques need to be applied in order to obtain constant angle domain data (Δt) from the uniformly time-sampled vibration data ($\Delta\theta$) [15,22].

As previously mentioned, the COT uses a resampling procedure which leads to an order domain spectrum instead of a frequency spectrum. In this paper, cubic spline interpolation was used to resample vibration signals from the time to angle domain. After resampling of the vibration signal from Fig. 11a, an order spectrum was derived (Fig. 13).

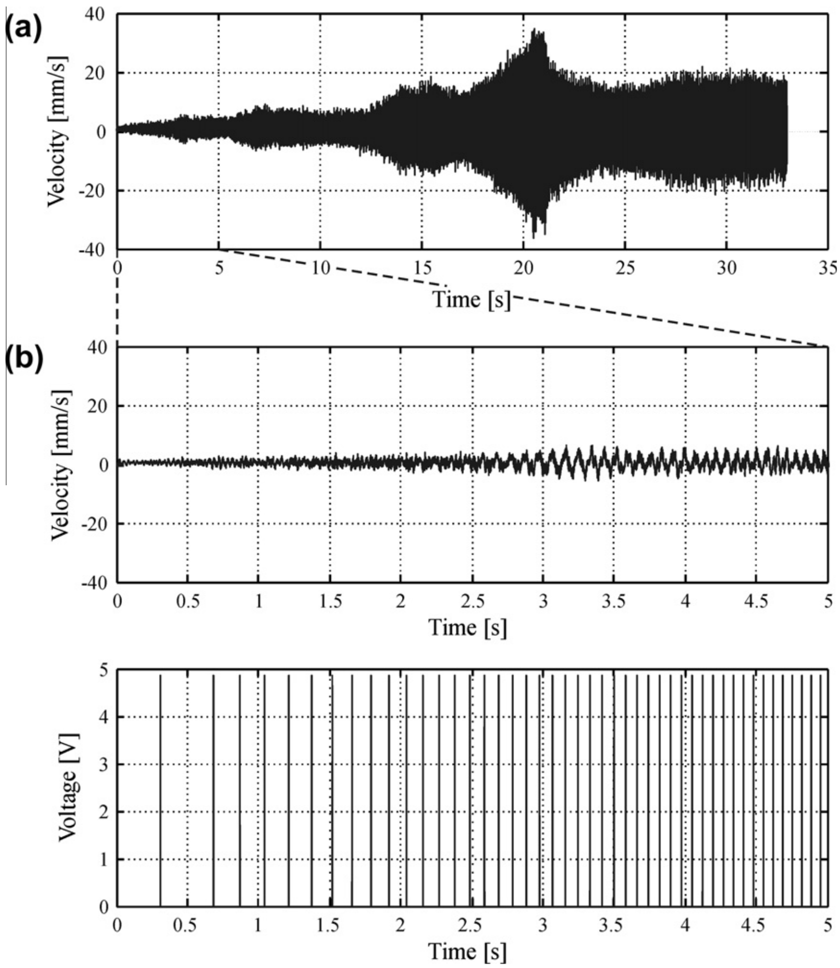

Fig. 11. Diagrams of signal change during run-up. (a) Vibration signal. (b) Partial vibration and key-phasor signal during a 0–5 s interval.

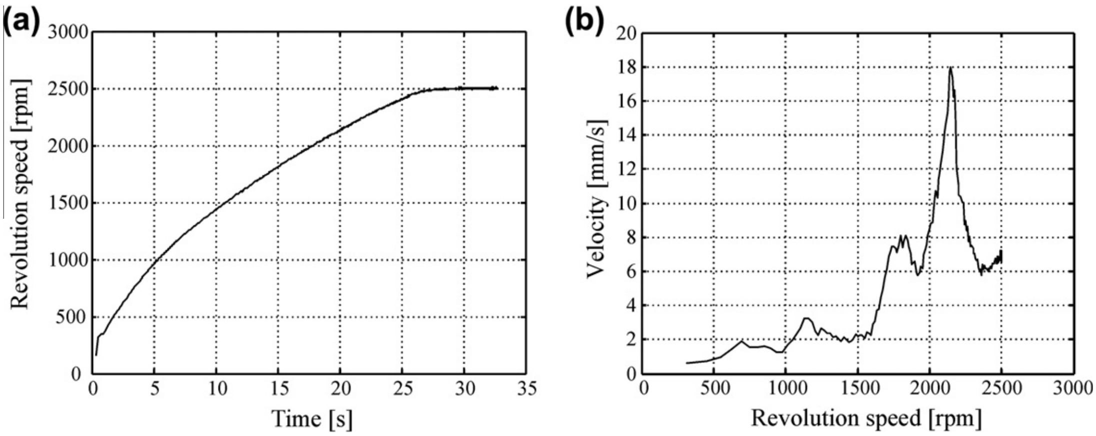

Fig. 12. Characteristic diagrams showing machine run-up. (a) Change of RPM. (b) Change of root mean square (rms) vibration velocity as the function of RPM at "E3" measurement spot.

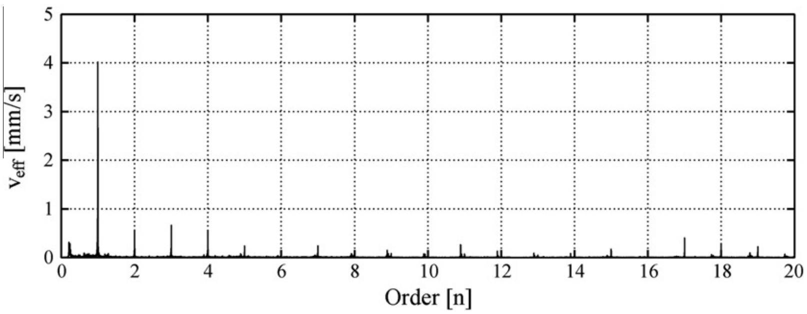

Fig. 13. Order spectrum.

As can be seen, the first order (1× rpm) is most dominant, but higher harmonics are also presented. Internal assembly looseness will produce higher harmonics due to the non-linear response of the loose parts to the excited forces from the rotating parts [9,23]. A misaligned bearing cocked on shaft [9] and angular shaft misalignment [6,9,23] will generate vibration frequencies of 1×, 2× and 3× rpm.

Additionally, the epicycle shafts can be considered as overhung rotors loaded by the cradle mass which causes static deflection of their axes. Therefore, these rotating elements are forced to rotate at high rotating speeds, while their rotating centre line does not coincide with the geometric centre line. Both rotors, on the left and right side, have significant rotating masses with opposite directions of rotation. This complex structure is loaded not only with static cradle mass, but also with dynamic forces which are generated during machine operation. Whenever the forced vibration frequency matches the natural frequency of a machine foundation, the amplitude rises significantly, much higher than expected compared to an unbalance effect, i.e., the resonance occurs [9]. This leads to extremely high vibrations, as in the case of the tested twisting machine.

6. Conducted activities in order to increase stiffness and improve the system's condition

As stated in the previous analysis, the cracks appeared due to a high concentration of stress in the crack zone, and misalignment of bearings, which, in turn, caused high loads on the foundation framework. Ultimately, this lead to the complete breakdown of the line for production of PP yarn, causing substantial financial losses. It was of utmost importance to quickly bring all twisting machines into a full operational state. Since time was a critical factor, and the small manipulation space limited options for reinforcement, and considering FEM analysis results, the following activities were undertaken (Fig. 14):

- foundation framework was reinforced using "P" support plates on both lateral sides of the bearings, and
- lower foundation framework was reinforced using a stable "UP" profile.

In order to transfer the loads from the upper foundation framework onto the lower part, and unload the lateral support plates on which the cracks appeared, the distance plates "D" were used to connect the "P" and "U" profile plates into a "UP" plate. Those reinforcement elements were welded together.

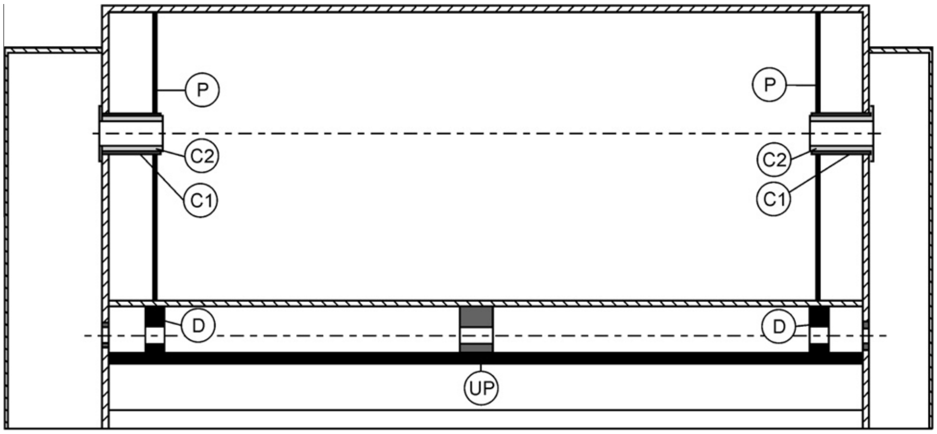

Fig. 14. Reinforcement zones within the foundation framework.

Once the reinforcement of the twisting machine foundation framework was finished, in order to minimise manufacturing errors, bushings ‘‘C1’’ in the framework assembly were counterbored, and bushings ‘‘C2’’ were chrome plated and grinded, while a number of other technological improvements were also made.

Due to limited time, and complexity of the cradle and epicycle assemblies, a number of technological improvements aimed to increase the twisting machines' reliability, had to be omitted.

Reinforcements were aimed at unloading the zones with high stress and displacement – ‘‘E1’’, ‘‘E2’’, and ‘‘E3’’ (Fig. 2), and preventing the growth of cracks in ‘‘E2’’ zones. FEM analysis and the results of vibration measurements showed that the added framework reinforced the foundation, rising the critical speed of the twisting machine above its operating RPM range.

7. An analysis of the effects of the redesign

The effects of the redesign of the twisting machine foundation framework are best discussed over the results of FEM analysis and measurement of vibration velocity in the critical zones (‘‘E1’’, ‘‘E2’’, and ‘‘E3’’). Axial (*Y*-axis) displacement in the crack zone of the lateral support plate (Fig. 15) was determined by numerical integration of the signal of vibration velocity in that zone. The method for measurement of vibrations was described in detail in Section 5. The calculated values of axial displacement in the crack zone were used as the input for FEM analysis and the calculation of stresses in the crack zone after the redesign. Fig. 15 compares peak-to-peak displacement in the crack zone, before and after the redesign.

Fig. 15 shows a significant reduction of radial displacement in the crack zone, due to redesign. Axial displacements of $\approx$100 μm peak-to-peak, i.e., ±0.05 mm (Fig. 15) in the crack zone, correspond to 2140 RPM, which represents approximately 90% of the maximum twisting machine capacity. The goal of FEM analysis is to determine the level of loads in the crack zone which correspond to that displacement.

Simulation of various load directions and senses in the radial *XZ*-plane, revealed that a horizontal static force of 4.5 kN (Fig. 16a and b) causes a displacement of -0.05023 mm (Fig. 17a and b) in the crack zone. This displacement corresponds to 2140 RPM working regime. Stress magnitudes are given in Fig. 16:

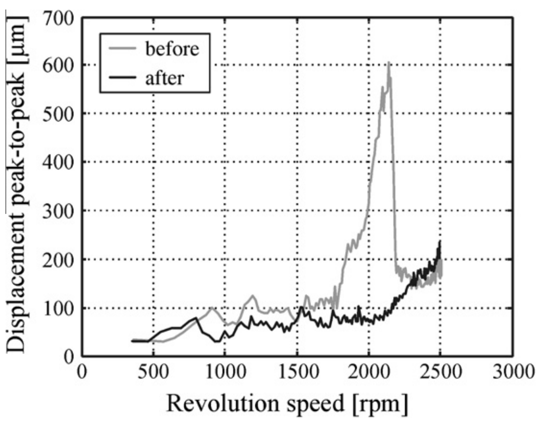

Fig. 15. Comparison of peak-to-peak displacement in axial direction in the crack zone of the lateral support plate, before, and after the redesign.

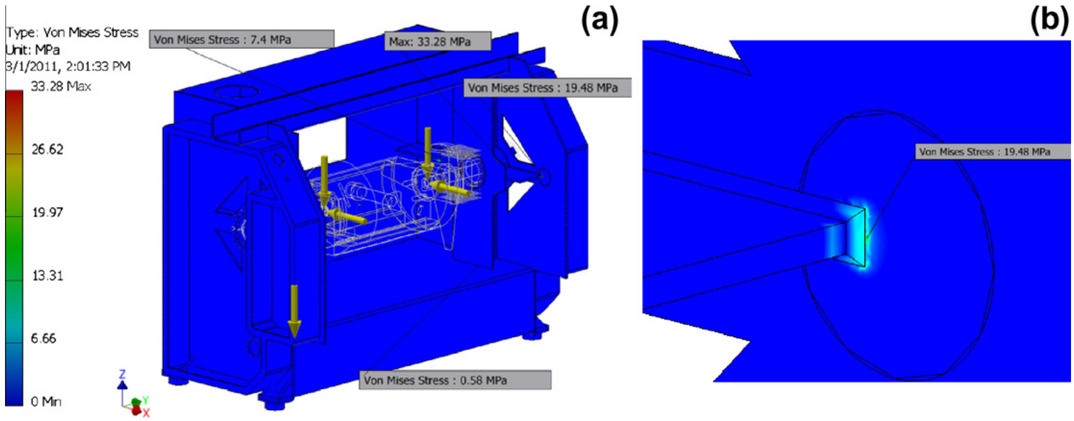

Fig. 16. (a) Distribution of Von-Mises stress in the redesigned twisting machine foundation framework. (b) A detail of the stress concentration zone.

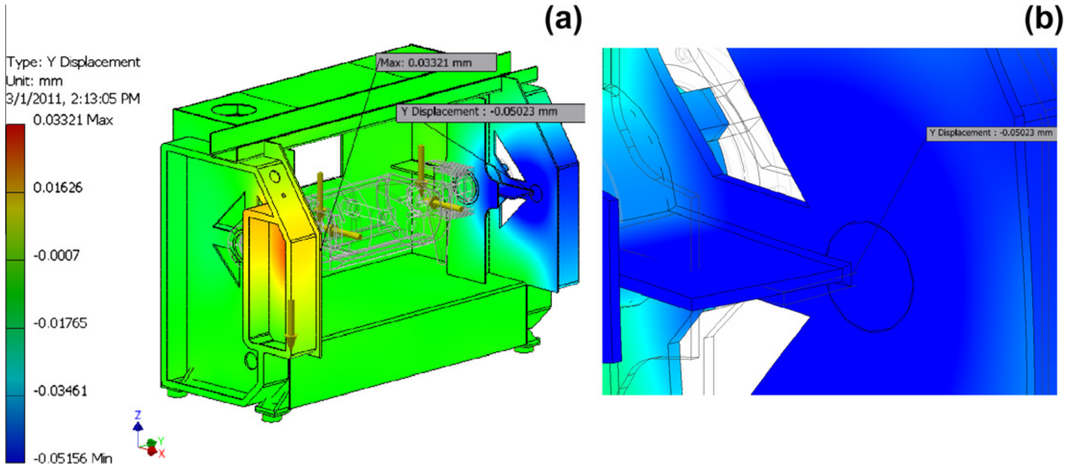

Fig. 17. (a) Displacement field in *Y*-axis direction after the redesign. (b) Detail of displacement field in the crack zone.

- crack zone, 19.48 MPa (zone "E2"),
- central bearing zone, 7.4 MPa (zone "E3"), and
- zone of vertical rib support, 0.58 MPa (zone "E1").

Simulation of various load directions revealed that the stress in zone "E3" reaches a maximum of 7.4 MPa for the load direction shown in Fig. 16. This is a seven times lower value compared to the stress before the redesign. The stress in zone "E1" is largest when the simulated load is vertical and superimposed with the cradle gravity force. In that case, the stress in zone "E1" equals 2.37 MPa, which is four times lower compared to the state prior to redesign. Considering the lower values of stress, graphical illustration of this analysis is omitted for the sake of brevity.

Shown in Fig. 17 are the displacements in a *Y*-axis direction on the lateral support plate. It should be noted that the *Y*-axis displacement of −0.05026 mm in the crack zone is very close to ±0.05 mm displacement obtained by the calculation of vibration velocity (Fig. 15).

The results of FEM analysis reveal that the redesign brought significant reductions of stress in the critical zones, especially in the crack zone, where the stress was reduced by more than eight times. Thus, one of the basic goals of redesign was fulfilled.

8. Results of vibration measurements

A comparative review of vibration velocity levels before and after the redesign of the twisting machine foundation framework are shown in Figs. 18–20.

The results of vibration measurements (Figs. 18–20) indicate significantly lower level of vibrations after the redesign, in all critical zones – especially the crack zone.

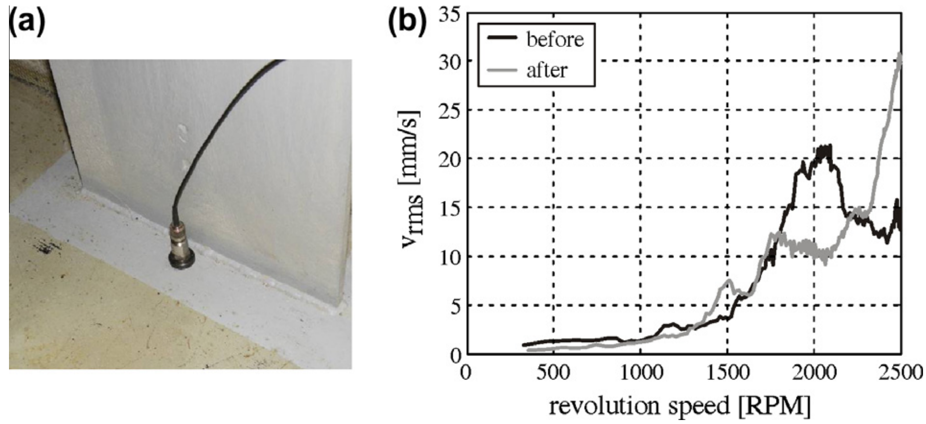

Fig. 18. Measurement spot in "E1" zone. (a) Photo of sensor. (b) Comparison between vibration levels before, and after the redesign.

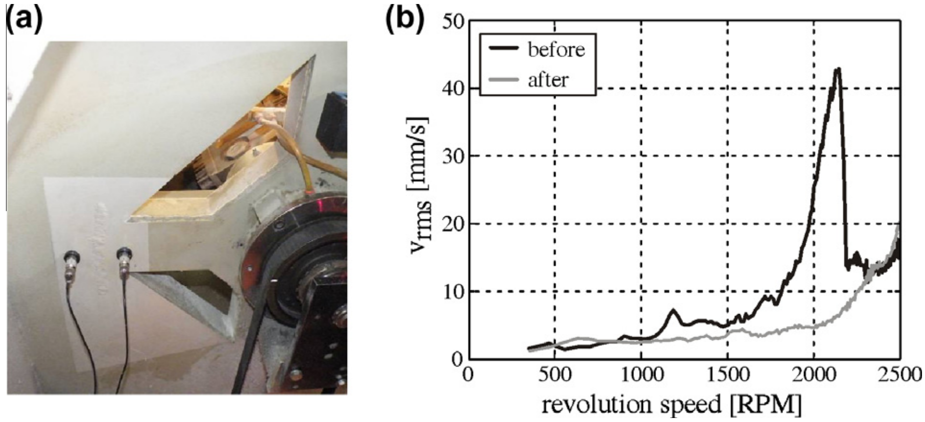

Fig. 19. Measurement spot in "E2" zone. (a) Photo of sensor. (b) Comparison between vibration levels before, and after the redesign.

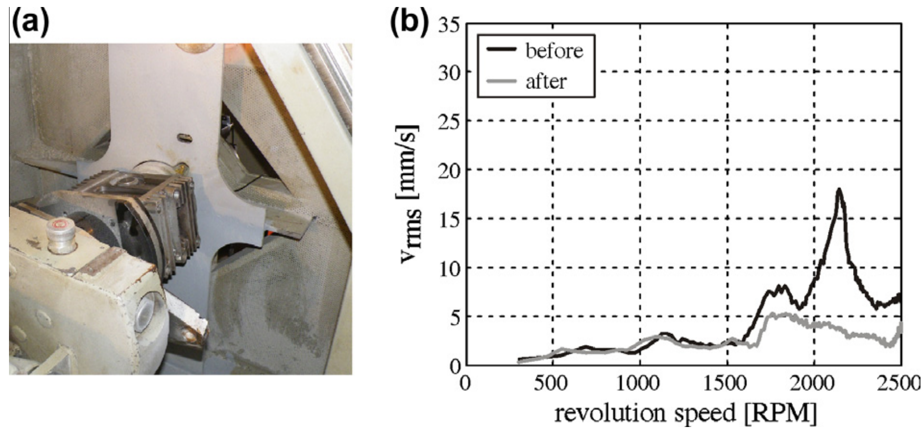

Fig. 20. Measurement spot in "E3" zone. (a) Photo of measurement spot. (b) Comparison between vibration levels before, and after the redesign.

9. Discussion

Stress analysis before and after the redesign of the foundation framework of the twisting machine leads to the conclusion that Von-Mises stress was reduced by more than eight times in the critical crack zone. FEM analysis also revealed significant drops in stress in other zones (zone "E1", and zone "E3"). The redesign contributed to the reduction of stress in zones "E1", and "E3", by more than four, i.e., six times, respectively.

Analysis of the results of vibration measurements, after the redesign, yields the conclusion that the redesign was very successful. At 2140 RPM (which corresponds to 90% of full load), the effects are as follows:

- In "E1" zone, the vibration velocity dropped from 20 mm/s to 12 mm/s. The resonance zone was shifted to around 2500 RPM, which is significantly above the operating regime.
- In "E2" zone, the vibration velocity dropped from 40 mm/s to 5 mm/s. This implies that the vibrations in the most critical zone (the crack zone) diminished by approximately eight times.
- In "E3" zone, the vibration velocity dropped from 15 mm/s to 3 mm/s, which means a decrease of vibration velocity in the zone of central bearing by about five times.

10. Conclusions

The analysis of a real technical system – a twisting machine, revealed a series of design flaws, manufacturing errors, and high vibration levels, cracks in the framework, and a breakdown of the PP yarn production line. In the course of restoring the twisting machine to full operational condition, the following were performed:

- Analysis of the foundation framework, which included videoscopic examination of cracks, measurement and analysis of manufacturing errors, definition of critical zones within the foundation framework, calculation of stress states and displacement by FEM analysis, and measurement of vibration in the critical zones.
- Framework redesign included not only the reinforcements of the critical zones, but also encompassed a number of technological procedures (counterboring of holes, chrome-plating of bushings, etc.) which were undertaken to reduce misalignment and inertial forces.
- Evaluation of the conducted redesign of the foundation framework through comparative analysis of vibration in the critical zones, before and after the improvement.

The results of FEM analysis which simulated loads and the stress field which correspond to measured and calculated displacements in the crack zone, before and after the redesign, revealed a significant drop in stress in the crack zone. More precisely, after completion of the redesign, the Von-Mises stress was decreased by more than eight times, indicating that the basic goal of unloading the most critical framework section was successfully accomplished.

The results of vibration measurement showed that the cracking zone (zone "E2"), bearing zone (zone "E3"), and support zone of the vertical rib (zone "E1") were unloaded. Based on the shown results it can be concluded that the redesign of the foundation framework of the twisting machine was successful. Owing to these measures, the examined twisting machine and all other machines were restored to their full operating capacity, which enabled the whole production line for PP thread to become fully operational.

The authors think that the relationship established between experimentally and theoretically defined displacements, and loads in the crack zone can be successfully used for analysis of complex technical systems which do not allow exact determination of framework loads.

References

[1] Todorovic P, Jeremic B, Macuzic I. Technical diagnostics, Faculty of Mechanical Engineering, Kragujevac; 2009 [In Serbian].
[2] Trebuna F, Simcak F, Bocko J, Trebuna P, Pastor M, Sarga P. Analysis of crack initiation in the press frame and innovation of the frame to ensure its further operation. Eng Fail Anal 2011;18:244–55.
[3] Witek L, Orkisz M, Wygonik P, Musili DN, Kowalski T. Fracture analysis of a turbine casing. Eng Fail Anal 2011;18:914–23.
[4] Goksenli A, Eryurek IB. Failure analysis of an elevator drive shaft. Eng Fail Anal 2009;16:1011–9.
[5] Poursaeidi E, Mohammadi Arhani MR. Failure investigation of an auxiliary steam turbine. Eng Fail Anal 2010;17:1328–36.
[6] Sinha JK, Lees AW, Friswell MI. Estimating unbalance and misalignment of a flexible rotating machine from a single run-down. J Sound Vib 2004;272:967–89.
[7] Lees AW, Sinha JK, Friswell MI. Model-based identification of rotating machines. Mech Syst Signal Process 2009;23:1884–93.
[8] Feng NS, Hahn EJ. Including foundation effects on the vibration behaviour of rotating machinery. Mech Syst Signal Process 1995;9:243–56.
[9] Girdhar P, Scheffer C. Practical machinery vibration analysis and predictive maintenance. Newnes: Elsevier; 2004.
[10] The European Committee for Standardization (CEN). EN 10025, Hot rolled products of structural steels; 2004.
[11] Budjevac D. Steel structural analysis and design, University of Belgrade, Belgrade; 1995 [In Serbian].
[12] Toribio J, Kharin V, Ayaso FJ, Gonzalez B, Matos JC, Vergara D, et al. Failure analysis of a lifting platform for tree pruning. Eng Fail Anal 2010;17:739–47.
[13] Gagg CR, Lewis PR. In-service fatigue failure of engineered products and structures – Case study review. Eng Fail Anal 2009;16:1775–93.
[14] Wang KS, Heyns PS. Application of computed order tracking. Vold-Kalman filtering and EMD in rotating machine vibration. Mech Syst Signal Process 2011;25:416–30.
[15] Fyfe KR, Munck EDS. Analysis of computed order tracking. Mech Syst Signal Process 1997;11:187–205.
[16] Beslak A, Flasker J. Detecting cracks in the tooth root of gears. Eng Fail Anal 2007;14:1466–75.
[17] Dahlquist G, Bjorck A. Numerical methods in scientific computing, Vol. I. Philadelphia: Society for Industrial and Applied Mathematics; 2008.
[18] Golub GH, Van Loan CF. Matrix computations. 3rd ed. Baltimore and London: The Johns Hopkins University Press; 1996.
[19] Brandt A, Lago T, Ahlin K, Tuma J. Main principles and limitations of current order tracking methods. Sound Vib 2005;39:19–22.
[20] Gade S, Herlufsen H, Konstantin-Hansen H, Wismer NJ. Order tracking analysis, technical review no. 2. Naerum: Bruel & Kjaer; 1995.
[21] Todorovic P, Jeremic B, Macuzic I, Brkovic A, Proso U. Vibration analysis of cracked rotor during run-up. Tribol Ind 2008;30:55–62.
[22] Blough JR. A survey of DSP methods for rotating machinery analysis. What is needed, what is available. J Sound Vib 2003;262:707–20.
[23] Mobley RK. Root cause failure analysis. Woburn MA: Butterworth-Heinemann/Elsevier; 1999.